JVI Journals.ASM.org

# A Single Amino Acid at the Hemagglutinin Cleavage Site Contributes to the Pathogenicity and Neurovirulence of H5N1 Influenza Virus in Mice

**Yi Zhang,[a] Yipeng Sun,[a] Honglei Sun,[a] Juan Pu,[a] Yuhai Bi,[b] Yi Shi,[b] Xishan Lu,[b] Jing Li,[c] Qingyu Zhu,[c] George F. Gao,[b] Hanchun Yang,[a] and Jinhua Liu[a]**

Key Laboratory of Animal Epidemiology and Zoonosis, Ministry of Agriculture, College of Veterinary Medicine, China Agricultural University, Beijing, China[a]; Chinese Academy of Sciences Key Laboratory of Pathogenic Microbiology and Immunology (CASPMI), Institute of Microbiology, Chinese Academy of Sciences, Beijing, China[b]; and State Key Laboratory of Pathogens and Bio-Security, Academy of Military Medical Sciences, Beijing, China[c]

**H5 influenza viruses containing a motif of multiple basic amino acids at the hemagglutinin (HA) cleavage site (HACS) are highly pathogenic in chicken but display different virulence phenotypes in mammals. Previous studies have shown that multiple basic amino acids of H5N1 influenza virus are a prerequisite for lethality in mice. However, it remains unclear which specific residue at the cleavage site affects the pathogenicity of H5N1 in mammals. A comprehensive genetic analysis of the H5N1 HACS showed that residues at P6 (position 325, by H3 numbering) were the most polymorphic, including serine (S), arginine (R), deletion (*), glycine (G), and isoleucine (I). To determine whether a single residue at P6 could affect virulence, we introduced different mutations at P6 of an avirulent clade 7 H5N1 strain, rg325G, by reverse genetics. Among the recombinant viruses, the rg325S virus showed the highest cleavage efficiency *in vitro*. All these viruses were highly pathogenic in chicken but exhibited different virulences in mice. The rg325S virus exhibited the highest pathogenicity in terms of unrestricted organ tropism and neurovirulence. Remarkably, the HA-325S substitution dramatically increased the pathogenicity of H5N1 viruses of other clades, including clades 2.2, 2.3.2, and 2.3.4, indicating that this residue impacts genetically divergent H5N1 viruses. An analysis of predicted structures containing these mutations showed that the cleavage site loop with 325S was the most exposed, which might be responsible for the efficient cleavage and high virulence. Our results demonstrate that an amino acid substitution at the P6 cleavage site alone could modulate the virulence of H5N1 in mice.**

The highly pathogenic H5N1 avian influenza viruses have undergone widespread geographic expansion among wild and domestic birds since they were first detected in the Guangdong Province of China in 1996 (3, 20, 24). They are deadly pathogens in chickens and humans and may cause a future influenza pandemic. As of 26 March 2012, 15 countries have reported 598 confirmed infections and 352 human deaths due to H5N1, which is due primarily to the transmission of the H5N1 virus from domestic poultry to humans (23). The threat posed by H5N1 to humans urges us to explore the molecular basis for pathogenicity in mammals.

An essential step in infection by influenza virus is the proteolytic processing of the trimeric hemagglutinin (HA) protein. The envelope glycoprotein HA precursor, HA0, requires proteolytic cleavage by cellular proteases into the subunits HA1 and HA2 to mediate fusion between the virion and endosomal membranes (21, 22). The nomenclature of the HA cleavage site (HACS) positions was designated previously, with cleavage occurring between P1 and P1′, with the position numbers increasing in the N-terminal direction along the cleaved peptide bond (P2, P3, and P4, etc.) (15). The cleavage activation of HA0 can be achieved by two classes of proteases. The first is lysine or arginine, favoring trypsin-like proteases, which exist in a limited number of cells or tissue types. The second is ubiquitously expressed subtilisin-like proteases (SLPs), which recognize a sequence of polybasic residues only (8). Highly pathogenic H5 and H7 subtype influenza viruses carry a polybasic HACS, leading to proteolytic activation by the ubiquitous protease furin (8, 17), resulting in unrestricted organ tropism and a highly pathogenic phenotype in poultry. The multiple basic amino acids at the cleavage site of the H5 subtype virus are also a prerequisite for lethality in mice (5). However, the specific amino acid(s) at or adjacent to HACS responsible for the virulent phenotype of H5N1 in mice remains unknown.

Previous reports have demonstrated that an amino acid change in the P2 position of the H1 cleavage site alone controls the virulence of A/WSN/33 virus (18). An analysis of multiple HACS sequences from H5N1 viruses available in databases revealed that the P6 position of the cleavage site was the most polymorphic. The P6 residue was an important feature of sequence recognition by proteases in the presence of a nearby carbohydrate side chain (7). We therefore sought to investigate the role of the residue at P6 in H5N1 virulence in mammals. We generated a series of cleavage site mutants with the backbone of an avirulent H5N1 virus, A/chicken/Sheny/0606/2008 (SY08), in mice by reverse genetics and characterized the reconstituted viruses *in vitro* and *in vivo*. Our results showed that the residue at the P6 cleavage position was related directly to the cleavage efficiency, replication, pathogenicity, and neurovirulence of H5N1 viruses in mice.

**Received** 17 December 2011 **Accepted** 3 April 2012
**Published ahead of print** 11 April 2012
Address correspondence to Jinhua Liu, ljh@cau.edu.cn.
Yi Zhang and Yipeng Sun contributed equally to this work.

doi:10.1128/JVI.07142-11

## MATERIALS AND METHODS

**Cells and virus.** Human embryonic kidney (293T) and Madin-Darby canine kidney (MDCK) cells were maintained in Dulbecco's modified Eagle's medium (DMEM; Life Technologies, Foster City, CA) supplemented with 10% fetal bovine serum (FBS; Life Technologies), 100 units/ml of penicillin, and 100 μg/ml of streptomycin. The SY08 (clade 7) and A/chicken/HB/0513/2007 (HB07) (clade 2.3.2) strains were isolated from cloacal swabs of apparently healthy chickens and passaged twice in 10-day-old specific-pathogen-free (SPF) chicken eggs. A/bar-headed goose/Qinghai/1/2005 (QH05) (clade 2.2) and A/tree sparrow/Jiangsu/1/2008 (JS08) (clade 2.3.4) were described previously (10, 11). All experiments with H5N1 influenza viruses were conducted in a biosecurity level 3 containment laboratory approved by the Biosafety Management Committee of the State Key Laboratory of Pathogens and Bio-Security.

**Generation of recombinant viruses by reverse genetics.** All eight gene segments amplified by reverse transcription-PCR (RT-PCR) from the SY08 virus were cloned into the dual-promoter plasmid pHW2000. Mutations (G325I, G325R, G325*, and G325S) were introduced into the HACS region by using a site-directed QuikChange mutagenesis kit (Agilent, Santa Clara, CA) according to the manufacturer's instructions. Primer sequences are available upon request. The reassortant viruses rg325G (wild type), rg325I, rg325R, rg325*, and rg325S were generated by reverse genetics (rg), as described previously (19). The rescued virus was detected by a hemagglutination assay. Viral RNA was extracted and analyzed by RT-PCR, and each viral segment was sequenced to confirm the identity of the virus. To determine the role of 325S in the virulence of H5N1 viruses of other clades, we constructed recombinant viruses with HA genes from the HB07, QH05, or JS08 virus in the SY08 backbone and introduced a 325S substitution into these recombinant viruses.

**Virus titration and replication kinetics.** The 50% tissue culture infectious dose ($TCID_{50}$) was determined in MDCK cells with 10-fold serially diluted virus inoculated at 37°C for 72 h. The 50% egg infectious dose ($EID_{50}$) was determined in 10-day-old embryonated chicken eggs with 10-fold serially diluted virus inoculated at 35°C for 48 h. The $TCID_{50}$ and $EID_{50}$ values were calculated by the method of Reed and Muench (13).

Multistep replication kinetics was determined by inoculating MDCK cells at a multiplicity of infection (MOI) of 0.001 $TCID_{50}$ per cell. Supernatants were sampled at 12, 24, 48, and 72 h postinoculation. Virus titers were determined by $TCID_{50}$ in MDCK cells. Three independent experiments were performed.

**Western blotting.** MDCK cells were inoculated with the wild-type or mutated virus at an MOI of 0.01 in the presence of either 2 μg/ml tosylsulfonyl phenylalanyl chloromethyl ketone (TPCK)-treated trypsin or no protease for 24 h in minimal essential medium containing 0.2% bovine serum albumin. Proteins from the supernatant were separated on 8% sodium dodecyl sulfate-polyacrylamide gel electrophoresis (SDS-PAGE) gels and then electrotransferred onto nitrocellulose membranes. Polyclonal mouse anti-HA antibody from A/bar-headed Goose/Qinghai/60/05 H5N1 expressed in baculovirus (1:2,500 dilution for 1 h at room temperature) was used to detect HA. Anti-influenza virus nucleoprotein monoclonal antibody (1:3,000 dilution for 1 h at room temperature; Abcam, Hong Kong) was used to detect NP. Goat anti-mouse IgG conjugated with horseradish peroxidase (1:5,000 dilution for 1 h at room temperature; Dingguo, Beijing, China) was used as a secondary antibody, followed by chemiluminescence detection (Supersignal West Pico chemiluminescent substrate kit; Pierce, Rockford, IL).

**Chicken studies.** The intravenous pathogenicity index (IVPI) of recombinant viruses was determined by using 10 6-week-old SPF White Leghorn chickens (Vital River Laboratory, Beijing, China) for each virus group, according to OIE standards (12). Chickens were injected intravenously in the ulnar vein with 0.1 ml of each virus at a dose of $10^6$ $EID_{50}$. Each bird was observed daily for clinical signs and was classified as healthy (score of 0), sick (exhibiting either respiratory symptoms, depression, diarrhea, cyanosis, edema, or nervous symptoms) (score of 1), severely sick (exhibiting severe or more than one of the above-mentioned symptoms) (score of 2), or dead (score of 3).

**Mouse studies.** Fifteen 6-week-old female BALB/c mice (Vital River Laboratory, Beijing, China) for each group were anesthetized with 20 μg/g tiletamine-zolazepam (Zoletil; Virbac) and inoculated intranasally with 50 μl of $10^6$ $EID_{50}$ of virus diluted in phosphate-buffered saline (PBS). Mock-infected control animals were inoculated intranasally (50 μl) with an equivalent dilution of noninfectious allantoic fluid. Three mice were euthanized on days 3 and 6 postinoculation (p.i.), respectively. Multiple organs, including lung, brain, liver, spleen, and kidney, were collected and homogenized in 1 ml of cold PBS. Virus titers in each organ were determined by inoculating 10-day-old embryonated chicken eggs with serial dilutions of virus.

A portion of the lung, brain, liver, spleen, and kidney of euthanized mice was preserved in 10% phosphate-buffered formalin on day 6 p.i. Samples were then processed for paraffin embedding and cut into 5-μm-thick sections. One section from each tissue sample was stained with hematoxylin and eosin (H&E) stain. Another section was processed for immunohistological staining with a mouse monoclonal antibody (AA5H; Abcam, Hong Kong) against influenza A virus NP and goat anti-mouse IgG biotin-conjugated affinity-purified antibody (Millipore, Billerica, MA). Specific antigen-antibody reactions were visualized by using diaminobenzidine-tetrahydrochloride (DAB) (Sigma, St. Louis, MO) and counterstained with hematoxylin.

The remaining five mice were monitored daily for clinical symptoms, weight loss, and mortality. Mice that lost more than 25% of their body weight were euthanized for humane reasons. The 50% minimum lethal dose ($MLD_{50}$) values were determined by intranasally inoculating groups of five mice with 10-fold dilutions of virus and were calculated by the method of Reed and Muench (13).

When we confirmed the role of 325S in the pathogenicity of H5N1 viruses of clades 2.2, 2.3.2, and 2.3.4, we inoculated 5 mice with $10^5$ $EID_{50}$ for each group. The mice were monitored daily for clinical symptoms, weight loss, and mortality.

**Statistical analyses.** Statistically significant differences between experimental groups were determined by using analysis of variance (ANOVA) with the GraphPad Prism software package (GraphPad Software Inc., La Jolla, CA). A $P$ value of less than 0.05 was considered statistically significant.

**Nucleotide sequence accession numbers.** The nucleotide sequences of the eight gene segments of SY08 are available from GenBank under accession numbers JQ277222 to JQ277229. The accession numbers for the HA gene are as follows: JQ809274 for HB07, AAZ17522 for QH05, and GQ202211 for JS08.

## RESULTS

**Bioinformatic analysis of the influenza virus H5 cleavage site.** A multiple-sequence alignment of the HA genes from H5N1 influenza viruses listed in the Influenza Information Resources of the World Health Organization (WHO) (http://www.who.int/influenza/resources) was performed. As shown in Table 1, the P1 positions of all the H5N1 viruses have an identical amino acid (arginine). The P2 to P5 cleavage site positions contain four basic amino acids, and the sequence is typically -R-R-K-K-. We found that the amino acid residues at position P6 varied. There were five different residues in this position, with different residues showing a clade preference. Most clade 7 viruses (78.6%) contained glycine; 95.7% of clade 5 viruses had isoleucine; and viruses of clades 0 (95.7%), 1 (84.0%), 2.1.1 (92.0%), 2.1.2 (100%), 2.2 (97.1%), 2.4 (92.0%), 3 (96.7%), 4 (100%), 6 (100%), 8 (100%), and 9 (100%) had arginine. The majority of clade 2.3 (98.4 to 100%) and 2.5 (71.4%) viruses had 1 amino acid deletion, and 79.2% of clade 2.1.3 viruses contained a serine at the P6 position.

**Generation of recombinant viruses.** To explore the influence

**TABLE 1** H5N1 influenza viruses possessing the corresponding HACS[a]

| Clade | No. of isolates | No. (%) of isolates with HACS | | | | | |
|---|---|---|---|---|---|---|---|
| | | GBBBBR ↓ G[b] | IBBBBR ↓ G[b] | RBBBBR ↓ G[b] | -BBBBR ↓ G[b] | SBBBBR ↓ G[b] | Other |
| 0 | 93 | 2 (2.2)[c] | 0 | 89 (95.7) | 2 (2.2) | 0 | 0 |
| 1 | 312 | 19 (6.1) | 0 | 262 (84.0) | 29 (9.3) | 0 | 2 (0.6) |
| 2.1.1 | 25 | 0 | 0 | 23 (92.0) | 1 (4.0) | 0 | 1 (4.0) |
| 2.1.2 | 34 | 0 | 0 | 34 (100) | 0 | 0 | 0 |
| 2.1.3 | 106 | 0 | 0 | 22 (20.8) | 0 | 84 (79.2) | 0 |
| 2.2 | 384 | 6 (1.6) | 0 | 376 (97.1) | 2 (0.5) | 0 | 0 |
| 2.3.1 | 13 | 0 | 0 | 0 | 13 (100) | 0 | 0 |
| 2.3.2 | 62 | 0 | 0 | 1 (1.6) | 61 (98.4) | 0 | 0 |
| 2.3.3 | 5 | 0 | 0 | 0 | 5 (100) | 0 | 0 |
| 2.3.4 | 115 | 0 | 0 | 0 | 115 (100) | 0 | 0 |
| 2.4 | 25 | 0 | 0 | 23 (92.0) | 2 (8.0) | 0 | 0 |
| 2.5 | 14 | 0 | 0 | 4 (28.6) | 10 (71.4) | 0 | 0 |
| 3 | 30 | 0 | 1 (3.3) | 29 (96.7) | 0 | 0 | 0 |
| 4 | 14 | 0 | 0 | 14 (100) | 0 | 0 | 0 |
| 5 | 23 | 0 | 22 (95.7) | 0 | 0 | 0 | 1 (4.3) |
| 6 | 4 | 0 | 0 | 4 (100) | 0 | 0 | 0 |
| 7 | 14 | 11 (78.6) | 0 | 1 (7.1) | 0 | 0 | 2 (14.3) |
| 8 | 4 | 0 | 0 | 4 (100) | 0 | 0 | 0 |
| 9 | 26 | 0 | 0 | 26 (100) | 0 | 0 | 0 |
| Total | 1,303 | 38 (2.9) | 23 (1.8) | 912 (70.0) | 240 (18.4) | 84 (6.4) | 6 (0.5) |

[a] Sequence data were obtained from the Influenza Information Resources of the WHO (http://www.who.int/influenza/resources).
[b] B, basic residue R/K. The sequences of more than 80% of the strains in the P5 to P2 positions were R-R-K-K-.
[c] Number of isolates possessing a specific amino acid at position P6 (proportion of isolates with a specific amino acid at position P6 in the H5N1 virus of the corresponding H5N1 clade in the Influenza Information Resources of the WHO database).

of the P6 cleavage position on the characteristics of H5N1 influenza viruses, we first established an eight-plasmid reverse genetics system for SY08 (rg325G), which is avirulent in mice. A series of mutants containing different amino acids (S, R, I, or a deletion) in the P6 position in the genetic backbone of rg325G was generated by site-directed mutagenesis. These mutants included rg325I, rg325R, rg325*, and rg325S (Table 2).

***In vitro* properties of H5N1 recombinant viruses.** The growth characteristics of H5N1 recombinant viruses were determined in eggs and MDCK cells. All of the HACS-mutated variants grew to significantly higher titers in eggs and MDCK cells than did the wild-type virus (rg325G) ($P < 0.01$) (Table 3). The yields of the HACS-mutated viruses were 0.9 to 1.2 logs and 0.9 to 1.5 logs higher than those of rg325G in eggs and in cell culture, respectively.

To further compare the replicative abilities of H5N1 recombinant viruses containing different HACSs, we assayed viral titers at different time points after infection in MDCK cells. As shown in Fig. 1A, the growth rate of rg325S was significantly higher than that of rg325G at 24, 48, and 72 h postinfection. The growth rates of rg325* and rg325R were significantly higher than that of rg325G at 24 and 72 h after infection, while the growth rate of rg325I was similar to that of rg325G at each time point. Taken together, our findings indicated that the mutant viruses, except for rg325I, possessed higher replicative abilities than the wild-type rg325G virus in *in vitro* systems.

To determine the influence of the P6 substitution on the activation of the cleavage of the HA precursor HA0, a Western blot analysis of supernatants from virus-infected MDCK cells was performed. The results showed that the HA0 of all the recombinant H5N1 viruses was cleaved completely dependent on exogenous trypsin. In contrast, HA0 precursors were cleaved into HA1 and HA2 fragments to various extents in the absence of exogenous trypsin. The recombinant virus rg325S showed the most efficient cleavage, whereas in other cases, cleavage was incomplete (Fig. 1B). Nevertheless, rg325R and rg325* displayed significantly more efficient cleavage than did rg325G and rg325I. These results indicated that the cleavage efficiencies of the recombinant viruses were consistent with their levels of replication in MDCK cells.

**Pathogenicity of H5N1 recombinant viruses in chicken.** To determine the virulences of recombinant viruses in natural hosts, we performed chicken IVPI tests. According to the criteria set by

**TABLE 2** Recombinant viruses with their HA cleavage site regions

| Virus | Description | HACS |
|---|---|---|
| rg325G | Dominant HACS sequence of clade 7 viruses | GRRKKR ↓ G |
| rg325I | Dominant HACS sequence of clade 5 viruses | IRRKKR ↓ G[a] |
| rg325R | Dominant HACS sequence of clade 0, 1, 2.1.1, 2.1.2, 2.2, 2.4, 3, 4, 6, 8, and 9 viruses | RRRKKR ↓ G |
| rg325* | Dominant HACS sequence of clade 2.3 and 2.5 viruses | *RRKKR ↓ G |
| rg325S | Dominant HACS sequence of clade 2.1.3 viruses | SRRKKR ↓ G |

[a] Underlining indicates the mutation at the P6 site.

**TABLE 3** *In vitro* characteristics and IVPI of the recombinant viruses

| Virus | Mean virus yield ± SD | | IVPI |
|---|---|---|---|
| | Eggs ($log_{10}$ $EID_{50}$/ml) | MDCK cells ($log_{10}$ $TCID_{50}$/ml) | |
| rg325G | 7.5 ± 0.3 | 4.5 ± 0.1 | 2.80 |
| rg325I | 8.5 ± 0.1 | 5.4 ± 0.4 | 2.84 |
| rg325* | 8.8 ± 0.1 | 5.6 ± 0.1 | 2.85 |
| rg325R | 8.5 ± 0.0 | 5.6 ± 0.2 | 2.91 |
| rg325S | 8.8 ± 0.1 | 5.6 ± 0.2 | 2.98 |

the OIE for the evaluation of pathogenesis in chickens, an avian influenza virus with an IVPI value greater than 1.2 is defined as highly pathogenic. Therefore, rg325G, rg325I, rg325*, rg325R, and rg325S, with IVPI values of 2.80, 2.84, 2.85, 2.91, and 2.98, respectively, were defined as highly pathogenic (Table 3).

**Pathogenicity of H5N1 recombinant viruses in mice.** To investigate virulence in mammals, we inoculated the recombinant viruses into a mouse model. Clinical signs and weight loss were evaluated after inoculating mice intranasally with $10^6$ $EID_{50}$ of each virus. Mice infected with rg325G or rg325I did not display obvious clinical signs during the course of the experiment. The weight of mice infected by rg325I was similar to that of mice infected with the mock control, while the weight of mice in the rg325G group increased after a slight initial reduction (Fig. 2A). In contrast, obvious clinical signs of disease were observed for mice infected with rg325*, rg325R, and rg325S from days 1 to 2 p.i. These signs included decreased activity, huddling, hunched posture, and ruffled fur. Moreover, these mice showed severe dyspnea starting at day 4 p.i., and obvious abdominal breathing was subsequently observed for some mice, in some cases resulting in death. A gross examination of dead mice revealed severe pneumonedema and pulmonary congestion. Survival curves clearly showed that rg325S had the highest pathogenicity, with an 80% mortality rate, followed by rg325* and rg325R, which caused 40% mortality in mice (Fig. 2B). There were no deaths among mice inoculated with rg325G or rg325I. The $MLD_{50}$ test also demonstrated that the pathogenicities of rg325*, rg325R, and rg325S were higher than those of rg325G and rg325I. Notably, rg325S was highly pathogenic in mice (Table 4).

**Replication of H5N1 recombinant viruses in mice.** Pathogenicity experiments with mice demonstrated that the virulences of rg325*, rg325R, and rg325S were obviously higher than those of the rg325G and rg325I viruses, and rg325S showed the highest virulence. To determine if the high pathogenicity resulted from enhanced replication, we inoculated groups of mice with $10^6$ $EID_{50}$ of each virus. The virus titers in lung, brain, liver, spleen, and kidney of three mice in each group were determined on days 3 and 6 p.i. (Table 4). The titers of rg325*, rg325R, and rg325S in lungs were significantly higher than those of rg325G on day 3 p.i., and the rg325S titer was significantly higher than that of rg325G on day 6 p.i. ($P < 0.05$). In contrast, the replication efficiency of rg325I was similar to that of rg325G. In general, the replication levels in lungs infected by the indicated viruses were consistent with their pathogenicity in mice. It should be noted that all recombinant viruses were restricted to the respiratory system, except for rg325S, which was detected in brain and spleen, indicating that the serine substitution at the P6 cleavage position may contribute to viral unrestricted organ tropism and neurovirulence in mice.

**Histopathology and IHC of recombinant H5N1 in mice.** To further examine viral pathology and tropism, we performed H&E staining and immunohistochemistry (IHC) on tissues from three mice from each group, collected on day 6 p.i. The rg325G and rg325I viruses induced mild interstitial pneumonia. Except for thickened alveolar walls with infiltrates of a few inflammatory cells and some edema, almost no lesions were observed for the rg325G and rg325I groups (Fig. 3A and B). Moderate interstitial pneumonia was observed for the lungs of mice infected with rg325* and rg325R, characterized by edema of the bronchial and vessel walls surrounded by massive inflammatory cells, including lymphocytes and monocytes, and desquamation of epithelial cells of the mucous membrane in the bronchial lumen (Fig. 3C and D). The rg325S-infected lungs exhibited the most severe lesions, with alveolar lumens and bronchioles flooded with edema fluid mixed with fibrin, erythrocytes, and inflammatory cells (Fig. 3E). Viral encephalitis was observed for the brains of mice infected with rg325S, characterized by spongiocyte infiltration (Fig. 3F). The rg325S virus also caused the rupture of brain blood vessels, resulting in a large number of red blood cells that infiltrated the brain (Fig. 3G). The immunohistochemical detection of influenza A virus nucleoprotein in the brain demonstrated that influenza virus antigen was found mainly in brain neurons (Fig. 3H). The histopathology and immunohistochemistry data further demonstrated

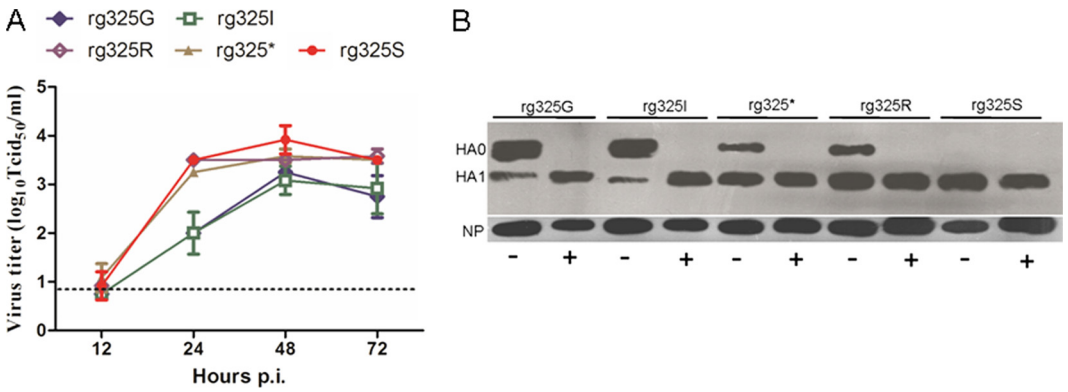


**FIG 1** *In vitro* replication properties of the recombinant viruses. (A) Multistep growth curves in MDCK cells. Error bars represent standard deviations from the means (SD) for three independent experiments. (B) Western blots of supernatants from infected MDCK cells incubated in the presence (+) or absence (−) of trypsin. Virus protein was detected with specific antibodies against HA or NP.

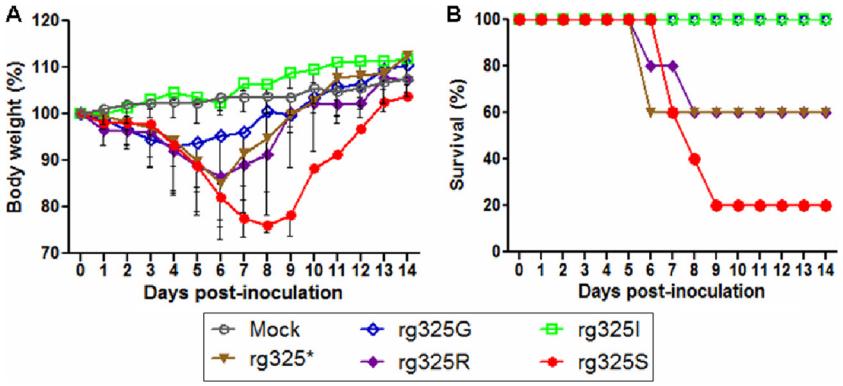


**FIG 2** Weight loss and mortality of mice inoculated with recombinant virus. Six-week-old female BALB/c mice ($n = 5$ mice/group) were inoculated intranasally with $10^6$ $EID_{50}$ of virus or diluent (mock). (A) The body weight of inoculated mice was measured daily and is represented as a percentage of the weight on the day of inoculation (day 0). The averages for each group are shown, and the error bars represent the SD. (B) The data show the survival percentages of mice infected with $10^6$ $EID_{50}$ of virus.

that the S mutation at P6 contributed to H5N1 neurovirulence in mice.

**Structural analysis of amino acid mutations in the HA protein.** To investigate the structural basis of the characteristics of H5N1 with different amino acids at the P6 HA cleavage position, we predicted HA monomer structures using the SWISS-Model website, employing the uncleaved H3 monomer as a template (2) (Fig. 4). We observed that the cleavage site loop with S or a deletion of an amino acid at the P6 HA cleavage position projects out from the glycoprotein surface. Compared with the deletion, the cleavage site loop with S at P6 was more exposed to the glycoprotein surface. With the exposed conformation, the potential proteases could more easily access the cleavage site loop. In contrast, the cleavage site loop with G, I, or R at the P6 position abuts the surface and is not exposed in the same way as when the deletion or S is evident, resulting in poor potential protease access. However, since R at P6 makes the loop more basic, the basic cleavage site loop could easily be cut by potential proteases at a low pH. This structural analysis supports our *in vitro* and *in vivo* observations.

**Role of HA-325S in conferring pathogenic properties of H5N1 viruses of other dominant clades.** To determine if HA-325S could alter the pathotypes of H5N1 viruses of other clades in mice, we constructed recombinant viruses with HA genes from the HB07 (clade 2.3.2), QH05 (clade 2.2), or JS08 (clade 2.3.4) virus in the SY08 backbone and introduced the 325S substitution to these recombinant viruses. Remarkably, the introduction of 325S into the HAs of these viruses increased morbidity and mortality (Fig. 5). rgQH05-R325S caused a higher mortality rate and a more rapid loss of body weight in mice than the wild-type virus (Fig. 5A and D). rgHB07-WT was not lethal to mice; in contrast, infection by rgHB07-*325S caused a significant loss of body weight and 60% mortality (Fig. 5B and E). The increase in pathogenicity caused by the HA-*325S substitution was more remarkable in the context of clade 2.3.4 HA. Infection with rgJS08-WT did not cause death or weight loss in mice; however, rgJS08-*325S resulted in 100% mortality by day 6 p.i. (Fig. 5C and F). These results indicated that 325S is a universal virulence marker for H5N1 influenza viruses.

## DISCUSSION

H5N1 influenza viruses have repeatedly infected humans and caused the deaths of more than 50% of the humans which they have infected, posing a potential global pandemic threat (20). However, the mechanism of the interspecies transmission of H5N1 viruses remains unclear. Although H5N1 viruses have not acquired human-to-human transmissibility, it is possible that they may adapt to humans through reassortment and/or by mutation. Investigations of factors related to host range and the virulence of H5N1 in mammals therefore have important implications for public health. The proteolytic processing of the trimeric HA is the first step in the infection of cells by influenza virus. The amino acids at the cleavage site play important roles in the recog-

**TABLE 4** Virulence of H5N1 recombinant viruses in mice

| Virus | $MLD_{50}$ | No. of infected mice/total no. of mice (mean virus titer in sample [$\log_{10}$ $EID_{50}$/ml] ± SD)[b] | | | | | | | | | |
|---|---|---|---|---|---|---|---|---|---|---|---|
| | | Lung | | Brain | | Liver | | Spleen | | Kidney | |
| | | 3 dpi[a] | 6 dpi | 3 dpi | 6 dpi | 3 dpi | 6 dpi | 3 dpi | 6 dpi | 3 dpi | 6 dpi |
| rg325G | >6.7 | 3/3 (3.5 ± 0.3) | 3/3 (2.5 ± 0.9) | 0/3 | 0/3 | 0/3 | 0/3 | 0/3 | 0/3 | 0/3 | 0/3 |
| rg325I | >7.7 | 3/3 (3.3 ± 1.1) | 3/3 (2.8 ± 0.9) | 0/3 | 0/3 | 0/3 | 0/3 | 0/3 | 0/3 | 0/3 | 0/3 |
| rg325* | 6.2 | 3/3 (5.1 ± 0.4)* | 3/3 (3.2 ± 0.7) | 0/3 | 0/3 | 0/3 | 0/3 | 0/3 | 0/3 | 0/3 | 0/3 |
| rg325R | 6.2 | 3/3 (5.4 ± 0.3)** | 3/3 (3.6 ± 1.0) | 0/3 | 0/3 | 0/3 | 0/3 | 0/3 | 0/3 | 0/3 | 0/3 |
| rg325S | 5.5 | 3/3 (5.8 ± 0.7)** | 3/3 (5.0 ± 0.7)** | 0/3 | 2/3 (1.8, 2.1)[c] | 0/3 | 0/3 | 1/3 (1.8)[c] | 0/3 | 0/3 | 0/3 |

[a] *, the lung titers of corresponding strains were significantly higher than those of rg325G, with a $P$ value of <0.05, as determined by ANOVA; **, the lung titers of the corresponding strains were significantly higher than those of rg325G ($P < 0.01$ by ANOVA).
[b] The lower limits of detection were $10^{1.2}$ $EID_{50}$/ml for lung and $10^{0.8}$ $EID_{50}$/ml for the other samples.
[c] The number(s) in parentheses shows the virus titer in an individual infected mouse.

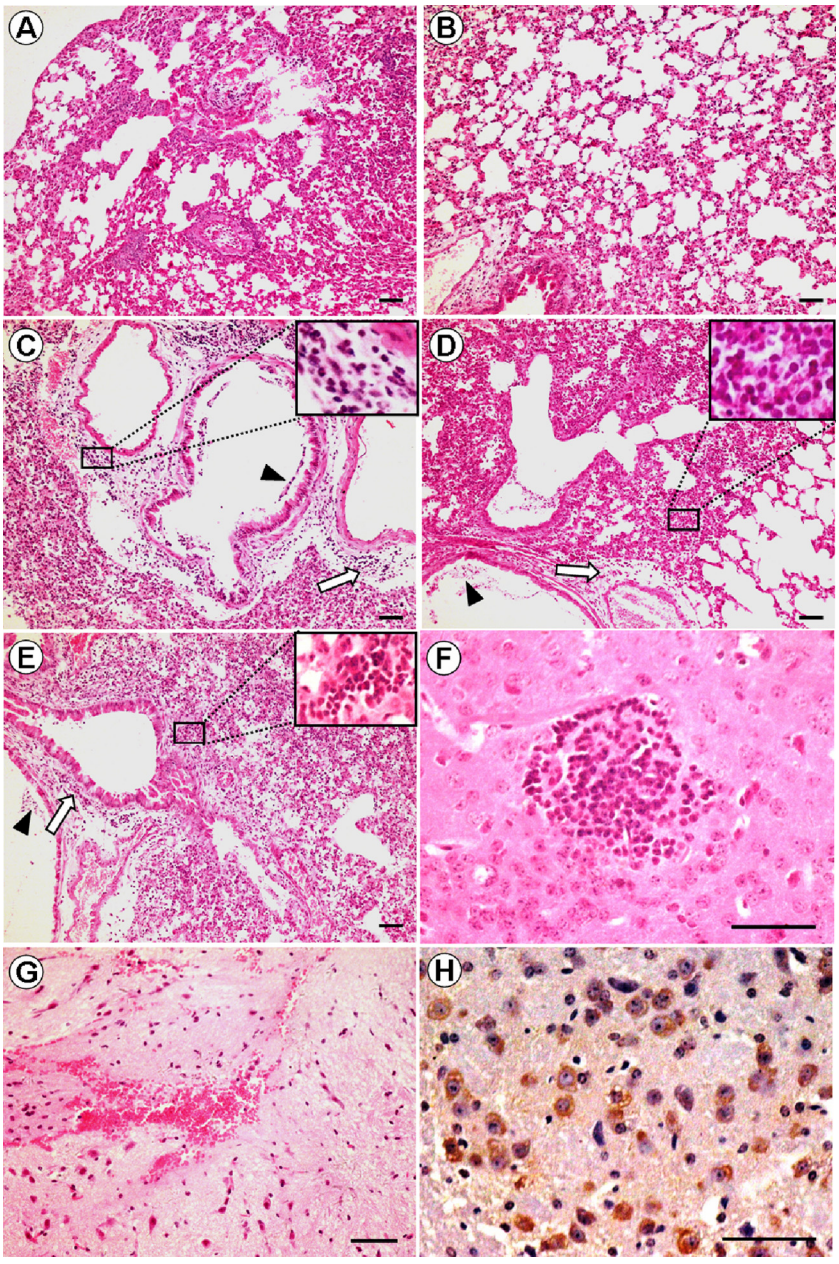


**FIG 3** Photomicrographs of hematoxylin-and-eosin (H&E)-stained and immunohistochemically stained tissue sections from mice on day 6 p.i. (A and B) rg325G virus (A) and rg325I virus (B) infections showing mild interstitial pneumonia with alveolar wall edema and thickening as well as inflammatory cell infiltration. (C and D) rg325* virus (C) and rg325R virus (D) infections showing moderate interstitial pneumonia; edema of the bronchial and vessel walls around inflammatory cells, including lymphocytes and monocytes (thick white arrow); and desquamation of epithelial cells of the mucous membrane in the bronchial lumen (triangle). (E) rg325S virus infection leads to diffuse alveolar damage; alveolar collapse; edema of the bronchial and vessel walls around inflammatory cells, including lymphocytes and monocytes (thick white arrow); desquamation of epithelial cells of the mucous membrane in the bronchial lumen (triangle); and inflammatory cell infiltrate with fibrinous exudates in the alveolar interstitial space. (F) rg325S virus infection leads to viral encephalitis, characterized by spongiocyte infiltration in the brain. (G) The rupture of brain blood vessels resulted in a large number of red blood cells infiltrating the brain. (H) Influenza virus antigen in brain neurons. Scale bars, 50 μm.

nition and binding of the protease as well as tissue tropism and pathogenicity in hosts. In this study, we present evidence that variation in position P6 of the HA cleavage site of an H5N1 influenza virus is linked directly to viral pathogenicity. Our results showed that a serine or arginine substitution or a deletion of glycine at the P6 cleavage site dramatically increases the replication ability and pathogenicity of SY08 in mice. In particular, a substitution of serine at position P6 results in unrestricted organ tropism and neurovirulence. Further mouse experiments showed that HA-325S increased the virulence of H5N1 viruses from other clades, including clades 2.2, 2.3.2, and 2.3.4.

Mutants were generated from SY08 with an amino acid deletion or substitution (G325I, G325R, or G325S), which frequently existed in H5N1 viruses at the P6 cleavage position. SY08, which

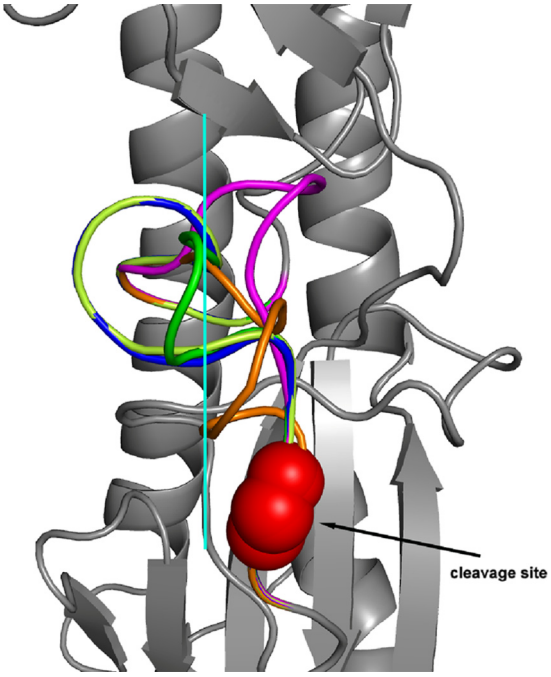


**FIG 4** Structural analysis of amino acid mutations at the P6 position of the HA cleavage site. Shown is a side view of the H3 HA trimeric structure based on A/Aichi/2/1968 (Protein Data Bank [PDB] accession number 1ha0) showing the different conformations of the cleavage site loops containing various amino acids at the P6 position (green, G; lemon, I; magenta, deletion; blue, R; orange, S). Red spheres represent the cleavage site, and the solid cyan line separates mutations into two groups based on the conformation.

was avirulent in mice, could cause the death of mice after a G325S or G325R substitution or a 1-residue deletion in this position but remained avirulent following the G325I substitution. Among these viruses, rg325S showed the highest virulence in mice, with an $MLD_{50}$ around 100-fold lower than that for rg235I. It is noteworthy that the HA-325S substitution in different clade (2.2, 2.3.2, and 2.3.4) HA backgrounds that are currently prevalent could also increase virulence in mice, indicating that HA-325S is a universal virulence marker of H5N1 virus in mice. In chickens, all the HACS mutants exhibited high pathogenicity because of the polybasic cleavage site. However, the pathogenicity of these viruses correlated with their virulence in mice. The IVPI of rg325S (2.98) was the highest among the viruses tested, followed by rg325R (IVPI of 2.91), rg325* (2.85), rg325I (2.84), and wild-type rg325G (2.80). These results demonstrate that mutations at the P6 cleavage position could influence the virulence of H5N1 influenza viruses in different species.

The results of the *in vitro* experiments showed that all of these mutations improved the replication ability of the wild-type virus in both eggs and MDCK cells. Mouse experiments showed that rg325*, rg325R, and rg325S, which exhibited higher pathogenicities than wild-type viruses, replicated more efficiently in lungs than did the wild-type virus. In contrast, the replication efficiency of rg325I, which was not lethal in mice, was similar to that of rg325G. These results suggest that the replication ability of these viruses is closely related to their pathogenicity. Since receptor-binding specificity could influence virulence in mice (25), we evaluated the receptor-binding specificity of the mutants. However, we did not observe any change in the receptor-binding specificity between wild-type and mutated viruses, and all of the viruses had only α-2.3 receptor-binding specificity (data not shown).

Our data suggest that the different cleavage efficiencies of viruses with P6 mutations might explain their replication levels and pathogenicities. The cleavage efficiencies of rg325*, rg325R, and rg325S were higher than those of rg325G and rg325I, and the cleavage of rg325S was the most efficient, revealing that the high cleavage efficiencies of rg325*, rg325R, and rg325S contributed to better replication and higher pathogenicity than those of the wild-type virus. The cleavage of HA is a prerequisite for viral infectivity (9). Horimoto and Kawaoka also demonstrated that the level at which HA is cleaved correlated with the degree of virulence when all other genetic characteristics were considered equal (6). To further investigate the mechanism for the different properties rendered by these mutations, we analyzed the structural basis of the different HACSs. Because there is no crystal structure of the uncleaved precursor of the H5 virus in the available databases, and the H5 uncleaved structure is similar to that of the H3 subtype (16), we used the HA0 structure of the H3 subtype as a template. An analysis of the HACS region predicted that the cleavage site

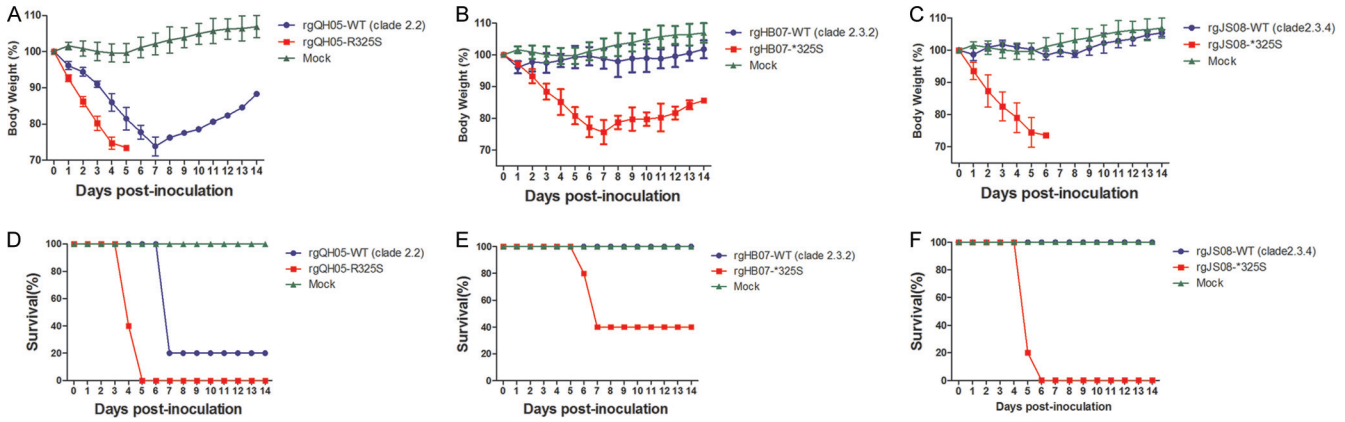


**FIG 5** Role of HA-325S in conferring the pathogenic properties of dominant H5N1 clades. Six-week-old female BALB/c mice ($n$ = 5 mice/group) were inoculated intranasally with $10^5$ $EID_{50}$ of virus or diluent (mock). (A to C) The body weights of inoculated mice were measured daily and are represented as a percentage of body weight on the day of inoculation (day 0). The averages for each group are shown, and the error bars represent the SD. (D to F) Survival data expressed as the percentage of mice infected with $10^5$ $EID_{50}$ of virus.

loop in 325S and 325* was more exposed at the glycoprotein surface than that in 325G, 325I, or 325R, allowing it to easily bind to potential proteases, favoring cleavage. However, since 325R results in a more basic loop than those of 325G and 325I, the basic cleavage site loop within 325R is also subject to potential proteases. These results explain the various virulence phenotypes of H5N1 viruses with mutations at the P6 position presented in our study. Additionally, a previous study also suggested that the degree of exposure of the cleavage site might alter cleavage properties and/or the fusion propensity, thereby resulting in an altered pathogenicity of influenza viruses (16). Based on theoretical considerations and experimental observations, we speculate that the structural traits of the HACS loop within 325S, 325R, and 325* are favorable for cleavage, resulting in efficient viral replication and further leading to increased pathogenicity.

SY08 was restricted to the respiratory system of mice but could be detected in the spleen and brain after the introduction of a G325S substitution, indicating that a serine at P6 could result in systemic infection and neurovirulence in mice. The cleavage of HA by cellular proteases is essential for virus spread and pathogenesis. Furin, an SLP, is ubiquitous in cells, and the ability of residues to bind to furin is related to viral pathogenicity. A previous analysis of binding energies indicated that furin selectivity is due predominantly to interactions with P1, P4, and P6 (4). Moreover, Remacle et al. previously used furin to cleave over 100 decapeptide sequences of human, bacterial, and viral proteins. Those researchers found that furin strongly preferred the presence of a serine at P6 and that efficient substrates most frequently exhibited a serine in this position (14). In the present study, we observed that rg325S exhibited efficient cleavage *in vitro*, along with the best replication ability *in vivo* and *in vitro* among the tested viruses, likely contributing to systemic infection and neurovirulence in mice.

HA-325S, which resulted in the highest pathogenicity in mice in the present study, is a unique residue of clade 2.1.3 viruses, which are predominant in Indonesia. Among the countries that have reported human H5N1 virus infections, Indonesia has the most cases and a significantly higher mortality rate (156 deaths/188 cases) than those reported by other countries (1, 23). With the present findings, we suggest that HA-325S might contribute to the virulence of clade 2.1.3 viruses in Indonesia. Whether 325S is related to severe H5N1 infection is worthy of further investigations.

In summary, we found that the amino acid at the P6 position of HACS was related directly to the HA cleavage efficiency, replication, and virulence of H5N1 influenza virus in multiple species, especially mammals. HA-325S dramatically increased the virulence of H5N1 viruses across different clades in mice. We propose that the amino acid at the P6 cleavage position could serve as an indicator for recognizing a virus with a potential public health risk and might help in the prediction and prevention of a pandemic that could emerge at the human-animal interface.

## ACKNOWLEDGMENTS

We thank Wenhai Feng for revising the manuscript. We also thank Qinghui Mu, Jingjing Wang, Kai Wei, Guanlong Xu, and Lijie Du for technical assistance.

This work was supported by the National Science Fund for Distinguished Young Scholars (no. 31025029) and the National Basic Research Program (973 Program) (no. 2011CB504702). G.F.G. is a leading principal investigator of the Innovative Research Group of the National Natural Science of Foundation of China (NSFC) (grant no. 81021003).

## REFERENCES

1. **Abdel-Ghafar AN, et al.** 2008. Update on avian influenza A (H5N1) virus infection in humans. N. Engl. J. Med. **358**:261–273.
2. **Chen J, et al.** 1998. Structure of the hemagglutinin precursor cleavage site, a determinant of influenza pathogenicity and the origin of the labile conformation. Cell **95**:409–417.
3. **Duan L, et al.** 2008. The development and genetic diversity of H5N1 influenza virus in China, 1996–2006. Virology **380**:243–254.
4. **Guo XL, Li L, Wei DQ, Zhu YS, Chou KC.** 2008. Cleavage mechanism of the H5N1 hemagglutinin by trypsin and furin. Amino Acids **35**:375–382.
5. **Hatta M, Gao P, Halfmann P, Kawaoka Y.** 2001. Molecular basis for high virulence of Hong Kong H5N1 influenza A viruses. Science **293**:1840–1842.
6. **Horimoto T, Kawaoka Y.** 1997. Biologic effects of introducing additional basic amino acid residues into the hemagglutinin cleavage site of a virulent avian influenza virus. Virus Res. **50**:35–40.
7. **Horimoto T, Kawaoka Y.** 1994. Reverse genetics provides direct evidence for a correlation of hemagglutinin cleavability and virulence of an avian influenza A virus. J. Virol. **68**:3120–3128.
8. **Kawaoka Y, Webster RG.** 1988. Sequence requirements for cleavage activation of influenza virus hemagglutinin expressed in mammalian cells. Proc. Natl. Acad. Sci. U. S. A. **85**:324–328.
9. **Klenk HD, Rott R, Orlich M, Blodorn J.** 1975. Activation of influenza A viruses by trypsin treatment. Virology **68**:426–439.
10. **Liu J, et al.** 2005. Highly pathogenic H5N1 influenza virus infection in migratory birds. Science **309**:1206.
11. **Liu Q, et al.** 2010. Characterization of a highly pathogenic avian influenza H5N1 clade 2.3.4 virus isolated from a tree sparrow. Virus Res. **147**:25–29.
12. **OIE.** 2011. Manual of diagnostic tests and vaccines for terrestrial animals. Office International des Epizooties, Paris, France.
13. **Reed LJ, Muench H.** 1938. A simple method for estimating fifty percent endpoints. Am. J. Hyg. (Lond.) **27**:493–497.
14. **Remacle AG, et al.** 2008. Substrate cleavage analysis of furin and related proprotein convertases. A comparative study. J. Biol. Chem. **283**:20897–20906.
15. **Schechter I, Berger A.** 1967. On the size of the active site in proteases. I. Papain. Biochem. Biophys. Res. Commun. **27**:157–162.
16. **Stevens J, et al.** 2004. Structure of the uncleaved human H1 hemagglutinin from the extinct 1918 influenza virus. Science **303**:1866–1870.
17. **Stieneke-Gröber A, et al.** 1992. Influenza virus hemagglutinin with multibasic cleavage site is activated by furin, a subtilisin-like endoprotease. EMBO J. **11**:2407–2414.
18. **Sun X, Tse LV, Ferguson AD, Whittaker GR.** 2010. Modifications to the hemagglutinin cleavage site control the virulence of a neurotropic H1N1 influenza virus. J. Virol. **84**:8683–8690.
19. **Sun Y, et al.** 2011. High genetic compatibility and increased pathogenicity of reassortants derived from avian H9N2 and pandemic H1N1/2009 influenza viruses. Proc. Natl. Acad. Sci. U. S. A. **108**:4164–4169.
20. **Webster RG, Govorkova EA.** 2006. H5N1 influenza—continuing evolution and spread. N. Engl. J. Med. **355**:2174–2177.
21. **White J, Kartenbeck J, Helenius A.** 1982. Membrane fusion activity of influenza virus. EMBO J. **1**:217–222.
22. **White J, Matlin K, Helenius A.** 1981. Cell fusion by Semliki Forest, influenza, and vesicular stomatitis viruses. J. Cell Biol. **89**:674–679.
23. **WHO.** 2012. Cumulative number of confirmed human cases of avian influenza A/(H5N1) reported to WHO, 2003–2012. World Health Organization, Geneva, Switzerland. http://www.who.int/influenza/human_animal_interface/H5N1_cumulative_table_archives/en/.
24. **Xu X, Subbarao, Cox NJ, Guo Y.** 1999. Genetic characterization of the pathogenic influenza A/Goose/Guangdong/1/96 (H5N1) virus: similarity of its hemagglutinin gene to those of H5N1 viruses from the 1997 outbreaks in Hong Kong. Virology **261**:15–19.
25. **Yen HL, et al.** 2009. Changes in H5N1 influenza virus hemagglutinin receptor binding domain affect systemic spread. Proc. Natl. Acad. Sci. U. S. A. **106**:286–291.